

# Heterochromatin protein 1 expression is reduced in human thyroid malignancy

Maria S Tretiakova<sup>1</sup>, Sarah D Bond<sup>2</sup>, David Wheeler<sup>2</sup>, Alejandro Contreras<sup>3</sup>, Masha Kocherginsky<sup>4</sup>, Todd G Kroll<sup>5</sup> and Tracy K Hale<sup>2</sup>

Owing to the loss of heterochromatin integrity that occurs during thyroid tumorigenesis, the expression of Heterochromatin Protein 1 isoforms HP1 $\alpha$  and HP1 $\beta$  was assessed by immunohistochemistry in 189 thyroid tumors and non-neoplastic tissues. Expression of HP1 $\beta$  was significantly decreased in all thyroid lesions, except in follicular adenomas, when compared with matched adjacent normal tissue. This loss of HP1 $\beta$  expression may in part be caused by microRNA dysregulation. An example is miR-205, a microRNA that is abundantly upregulated in thyroid carcinomas and shown to reduce the expression of HP1 $\beta$ . In contrast to HP1 $\beta$ , HP1 $\alpha$  expression was only reduced in metastatic carcinomas and poorly differentiated lesions. These results suggest the reduction of HP1 $\beta$  followed by a decrease in HP1 $\alpha$  contributes to the pathogenesis of thyroid carcinomas, and their loss is a potential marker of thyroid malignancy and metastatic potential, respectively.

*Laboratory Investigation* (2014) 94, 788–795; doi:10.1038/labinvest.2014.68; published online 19 May 2014

**KEYWORDS:** heterochromatin protein 1; thyroid; microRNA

During malignant transformation nuclear architecture becomes more disorganized, with observable changes occurring in heterochromatin aggregation.<sup>1</sup> The human genome encodes three Heterochromatin Protein 1 (HP1) isoforms ( $\alpha$ ,  $\beta$ , and  $\gamma$ ), which are essential chromatin packaging proteins that function to restrict chromatin plasticity.<sup>2</sup> HP1 $\alpha$  and HP1 $\beta$  are the isoforms found in heterochromatin and are primarily associated with gene repression. Although generally ubiquitous in normal tissue, differential expression of each HP1 isoform has been observed in both human tumor derived tissues and cells.<sup>3–9</sup> The pattern of expression for HP1 isoforms in solid tumors appears to vary with the tumor context.<sup>3,5,7,9,10</sup> Loss of HP1 $\beta$  expression has been reported in poorly differentiated colon cancers, invasive melanoma lesions, and prostate cancer.<sup>11–13</sup> Loss of HP1 $\alpha$  expression has been observed in metastatic lesions,<sup>5</sup> and in medulloblastomas and advanced papillary thyroid carcinomas with poor outcome.<sup>7,9</sup> However, increased HP1 $\alpha$  has also been observed in a variety of solid tumors compared with non-tumor tissue.<sup>3</sup>

Thyroid neoplastic lesions range from benign follicular adenomas to malignant but relatively indolent papillary or

follicular carcinomas, and to the highly aggressive poorly differentiated or undifferentiated anaplastic carcinomas. Both papillary and follicular well-differentiated carcinomas, comprised of differentiated follicular cells, may metastasize or give rise to the undifferentiated anaplastic carcinomas that have a poor outcome.<sup>14,15</sup> Preoperatively, a common diagnostic problem is distinguishing between benign and malignant thyroid nodules, as this will influence management. Therefore, identifying specific markers that can be useful in improving the accuracy of diagnosis and predicting tumor behavior is of utmost priority.

A myriad of alterations occur at the molecular level across this spectrum of thyroid lesions causing the dysregulation of gene and microRNA (miRNA) expression.<sup>16</sup> It has been proposed that of the miRNAs that are dysregulated only those which are highly overexpressed or strongly down-regulated are involved in thyroid tumorigenesis.<sup>17</sup> Thyroid cancers exhibit aberrant miRNA expression that leads to the altered expression of oncogenes as well as tumor suppressor genes.<sup>17,18</sup> Interestingly, several miRNAs that are differentially upregulated in thyroid lesions are also predicted to target the HP1 family.<sup>19</sup>

<sup>1</sup>Department of Pathology, University of Washington, Seattle, WA, USA; <sup>2</sup>Institute of Fundamental Sciences, Massey University, Palmerston North, New Zealand; <sup>3</sup>Lester and Sue Smith Breast Center and the Department of Pathology, Baylor College of Medicine, Houston, TX, USA; <sup>4</sup>Department of Health Studies, University of Chicago, Chicago, IL, USA and <sup>5</sup>Department of Pathology, University of Chicago, Chicago, IL, USA

Correspondence: Dr TKG Hale, PhD, Institute of Fundamental Sciences, Massey University, Private Bag 11-222, Palmerston North 4442, New Zealand.  
E-mail: T.K.Hale@massey.ac.nz

Received 22 October 2013; revised 1 April 2014; accepted 13 April 2014

The need for improved accuracy in the diagnosis of thyroid lesions has led us to explore the expression of HP1 $\alpha$  and HP1 $\beta$  across benign and malignant thyroid tumors, respectively. Screening of a thyroid tumor tissue microarray (TMA) demonstrated that HP1 $\alpha$  expression was reduced in more advanced thyroid carcinomas, but was unchanged in well-differentiated thyroid neoplasms when compared with normal thyroid tissue. However, when compared with normal thyroid tissue, HP1 $\beta$  expression was significantly decreased in all thyroid neoplasms ( $P < 0.01$ ), except in follicular adenomas. Results indicate that a significant loss of HP1 $\beta$  may confer a malignant potential. We show that loss of HP1 $\beta$  could in part be due to the upregulation of specific miRNAs that are observed in thyroid tumors. These results suggest that the differential loss of HP1 $\alpha$  and HP1 $\beta$  represents potential molecular markers for different stages of thyroid malignancy.

## MATERIALS AND METHODS

### Tissue Microarrays

TMAAs were constructed using 189 formalin-fixed paraffin-embedded tissue blocks from 103 patients with benign and malignant thyroid tumors. Histological classification was based on diagnostic reports and slide re-reviews by two experienced pathologists (T Kroll and M Tretiakova). Questionable cases were not selected for inclusion. Hematoxylin and eosin-stained sections from lobectomy, partial and total thyroidectomy specimens were analyzed to define representative lesional regions and normal adjacent thyroid tissue regions. From these regions, a minimum of two duplicate tissue cylinders with a diameter of 1 mm were obtained and arrayed into recipient blocks using an automated tissue microarrayer (ATA-27, Beecher Instruments, Sun Prairie, WI, USA). The distribution of tissues was as follows: colloid nodules ( $N=5$ ), follicular adenoma ( $N=18$ ), Hurthle cell adenoma ( $N=10$ ), follicular carcinoma primary ( $N=14$ ) and metastases ( $N=8$ ), Hurthle cell carcinoma ( $N=8$ ), papillary carcinoma primary ( $N=32$ ) and metastases ( $N=3$ ), poorly differentiated ( $N=4$ ) and anaplastic carcinoma ( $N=7$ ), and normal matched adjacent thyroid tissue ( $N=80$ ). Recipient blocks were cut into 4- $\mu$ m-thick sections on Surgipath silane-coated positively charged slides for better adhesion and subjected to immunohistochemistry.

Fresh frozen, matched thyroid normal and papillary carcinoma tissue from four patients was obtained from Christchurch Cancer Society Tissue Bank, Christchurch, New Zealand. This study was approved by the New Zealand Upper South B Regional Ethics Committee and the University of Chicago Institutional Review Board.

### Antibodies

The primary antibodies used for this study were the HP1 $\alpha$  (C7F11) rabbit monoclonal antibody (Cell Signaling Technology, Danvers, MA, USA), HP1 $\beta$  (MAC353) rat monoclonal

antibody (Abcam, Cambridge, MA, USA), and  $\alpha$ -tubulin rat monoclonal antibody (Abcam).

### Immunohistochemistry

Immunohistochemical staining was performed using HRP-labeled dextrose-based polymer complex bound to secondary antibody EnVision (Peroxidase/DAB+) from DAKO (Glostrup, Denmark). After deparaffinization and rehydration, slides were blocked for endogenous peroxidase with 3% H<sub>2</sub>O<sub>2</sub> for 15 min at room temperature (RT), and then washed in Tris-buffered saline (TBS). Antigen retrieval was carried out by heating sections either in Tris-EDTA buffer (pH 9.0) for 15 min in a microwave oven or in 0.1 M citrate buffer (pH 6.0) for 3 min in a pressure cooker. Non-specific binding sites were blocked using Protein Block (DAKO) for 20 min at RT in a moist chamber. Then slides were incubated, at RT for 1 h or at 4 °C in a moist chamber overnight, with the HP1 $\alpha$  (1:200) or HP1 $\beta$  (1:300) antibodies diluted in Antibody Diluent (DAKO) as indicated. After TBS washes, staining was detected with EnVision system (DAKO) developed for 5 min with 3-3'-diaminobenzidine chromogen, counterstained with hematoxylin, and coverslipped. Negative controls were performed by substituting the primary antibody with non-immune mouse immunoglobulins.

### Evaluation of Immunostaining

Only nuclear labeling was accepted as specific for HP1. Nuclear expression was quantified manually using 200–500 cells at  $\times 400$  magnification, as well as by using Chromavision Automated Cellular Imaging System (ACIS, Clariant Inc, Aliso Viejo, CA, USA). Manual nuclear intensity scoring was graded semiquantitatively as negative (0), weak (1+), moderate (2+), or intense (3+) for each case. Automated ACIS scoring was applied to derive both intensity and percentage staining as previously described.<sup>20</sup> In brief, nuclear staining for HP1 was quantified based on three-color parameters: hue, luminosity, and saturation. Positive brown nuclear staining was recorded as a numerical score between 0 and 225 for each pixel and normalized to an area of 1  $\mu$ m<sup>2</sup>. In addition, the ACIS software was instructed by setting color-specific thresholds to determine brown (positive stain) from blue (negative counterstain) in the nuclei within each TMA core, and calculate the percent of nuclear positivity.

### Statistical Analysis

Statistical analysis was performed using STATA (College Station, TX, USA) software package. Nuclear expression levels were calculated as the mean of duplicate measurements  $\pm$  s.d.  $P$ -values were calculated using a two-tailed Student's  $t$  test for continuous variables. Correlations were calculated using the Spearman rank correlation test unless otherwise indicated.  $P < 0.05$  was considered to be statistically significant. Microarray data from GEO project GSE3467 was analyzed using the websites (<http://www.ncbi.nlm.nih.gov/geo/>) GEO2R application with the default settings.

### Cell Culture

The Nthy-ori 3-1 cell line (ECACC, Wiltshire, UK), derived from the normal thyroid follicular epithelial tissue of an adult that had been immortalized with SV40 large T antigen, was maintained in RPMI 1640 with 10% fetal bovine serum, 1% Penicillin/Streptomycin (Life Technologies, Grand Island, NY, USA) at 37 °C with 5% CO<sub>2</sub> in a humidified atmosphere.

### Transfection with Pre-miR miRNA Precursors

Nthy-ori 3-1 cells were transfected with 30 nM Pre-miR miRNA Precursors (Life Technologies) using X-tremeGENE siRNA Reagent (Roche Applied Science, Indianapolis, IN, USA) and Opti-MEM medium (Life Technologies). Media was replaced 24 h post transfection. Cells were plated at a density of  $8.5 \times 10^3$  cells/cm<sup>2</sup> to permit growth, without reaching confluency after 72 h.

### HP1 $\beta$ 3' UTR Luciferase Reporter Assay

pMIR-REPORT luciferase vectors (Life Technologies) harboring HP1 $\beta$  3' UTR sequences with a wild-type (pMIR-REPORT-HP1 $\beta$  WT) or mutated (pMIR-REPORT-HP1 $\beta$  Mut) predicted miR-205 binding site were generated. Annealed oligonucleotides, spanning the region from 240 to 290 bp of the HP1 $\beta$  3' UTR, that contained either a WT or Mut miR-205 seed region were cloned into the HindIII and SpeI restriction sites of the pMIR-REPORT vector. The sequences are shown in Figure 4a.

Nthy-ori 3-1 cells were co-transfected, as above, with the 5 nM Pre-miR miRNA Precursors (Life Technologies) and either 150 ng pMIR-REPORT-HP1 $\beta$  WT or Mut vector along with 100 ng pMIR-REPORT  $\beta$ -galactosidase control plasmid (Life Technologies). After 30 h, luciferase measurements were performed using the Luciferase Reporter Assay System (Promega, Madison, WI, USA). Firefly luciferase activity was normalized to  $\beta$ -galactosidase activity.

### Protein Extraction

Total protein was isolated from frozen matched thyroid normal and papillary carcinoma tissue (31–82 mg) using the mirVana Paris Kit (Life Technologies). The frozen tissue was placed in cold cell disruption buffer supplemented with Complete Protease inhibitor (Roche Applied Science) and homogenized on a Retsch MM301 tissue mill at 1000 rpm for 10 min, then incubated for 10 min at 4 °C. The supernatant was collected after centrifugation at 10 000 g at 4 °C.

Total protein from the Nthy-ori 3-1 cell line was obtained by washing cells twice in PBS, incubating the cells in cold lysis buffer (50 mM HEPES pH 8.0, 400 mM NaCl, 1% NP40, Complete Protease Inhibitor) then collecting the supernatant as above. The protein concentration was determined using the BCA Protein Assay Kit (Thermo Scientific, Rockford, IL, USA).

### Immunoblot Analysis

Samples were resolved by SDS-PAGE and then transferred to nitrocellulose. The blots were blocked for 1 h at RT with 5% BSA in 25 mM Tris, 150 mM NaCl pH 7.6 and 0.1% Tween-20 (TBS-T), then incubated with antibodies against, either HP1 $\alpha$ , HP1 $\beta$  or  $\alpha$ -tubulin in 5% BSA/TBS-T for 18 h at 4 °C. Blots were then washed four times in TBS-T, incubated 1 h at RT with the appropriate ECL HRP-linked whole secondary antibody (GE Healthcare, Buckinghamshire, UK) diluted in 5% BSA/TBS-T and washed as before, then developed with ECLplus Western Blotting Detection (GE Healthcare).

## RESULTS

### HP1 $\alpha$ Expression is Reduced in Metastatic Thyroid Neoplasms

To determine the level of HP1 $\alpha$  protein expression in thyroid tumors, a TMA containing 189 thyroid lesions and normal adjacent thyroid tissue was screened for HP1 $\alpha$  expression by immunohistochemistry. To ensure our results were representative of each tumor, the nuclear expression of HP1 was quantified manually by grading 2–3 cores, from 0 (negative) to 3+ (intense), and then averaging to give the intensity of HP1 staining for each tissue. The results are graphed in Figure 1a, with representative tissue sections shown in Figure 1b. The expression of HP1 $\alpha$  in carcinomas was comparable to that observed in normal tissue (Figure 1a), whereas HP1 $\alpha$  protein levels were slightly increased in adenomas compared with normal tissue and colloid nodules. A reduction of HP1 $\alpha$  expression was observed in metastatic and anaplastic variants, however, this was not significant when compared with normal tissue. When the carcinomas were divided into non-metastatic (primary) and metastatic (either regional or distal) groups, a significant reduction ( $P < 0.05$ ) in HP1 $\alpha$  expression was observed between papillary carcinomas and their metastatic counterparts (Figure 1c).

### Differential Loss of HP1 $\beta$ Expression in Thyroid Lesions

The thyroid TMA was also screened for HP1 $\beta$  protein expression and graded as described above. Normal thyroid tissue that demonstrated strong HP1 $\beta$  nuclear positivity served as a positive control. HP1 $\beta$  expression was significantly decreased ( $P < 0.01$ ) in all thyroid lesions, except follicular adenomas and colloid nodules, when compared with normal thyroid tissue by manual scoring for intensity of staining (Figures 2a and b).

Automated HP1 $\beta$  scoring similarly showed a significant decrease in both percent of nuclear positivity and staining intensity for all lesional tissues except follicular adenoma ( $P < 0.001$ , Table 1). Group comparison showed significant differences in staining intensity between normal/benign and malignant lesions with gradual loss of HP1 $\beta$  with malignant progression ( $P < 0.001$ ). We found a strong positive correlation between automated and semiquantitative manual grading of nuclear intensities for HP1 $\beta$  ( $r = 0.62$ – $0.75$ ).

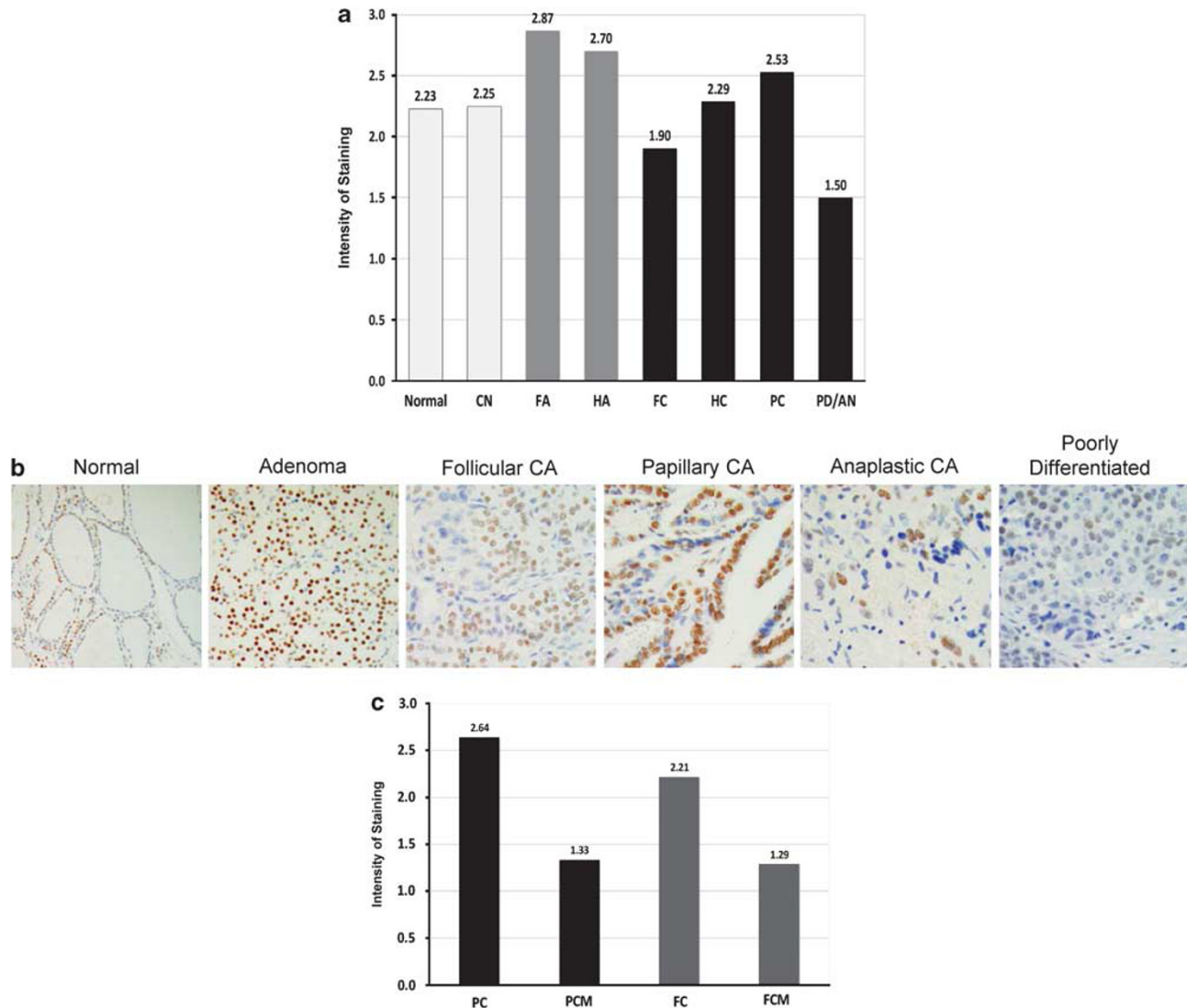


**Figure 1** Reduction of HP1 $\alpha$  expression in metastatic thyroid carcinomas. **(a)** Graph showing the results from immunohistochemical staining of a 189 sample human thyroid tumor TMA for HP1 $\alpha$ . The intensity of HP1 staining was graded as 0, 1+, 2+, and 3+. Colloid nodules (CN), follicular adenomas (FA), Hurthle cell adenomas (HA), follicular carcinomas (FC), Hurthle cell carcinomas (HC), papillary carcinomas (PC), poorly differentiated and anaplastic tumors (PD/AN), and normal adjacent thyroid tissue were stained. **(b)** Representative images from the immunohistochemical staining of the human thyroid tumor TMA are shown for HP1 $\alpha$ . Haematoxylin counterstaining (blue) indicates nuclei, HP1 $\alpha$  positive nuclei (brown). CA, carcinoma. Original magnification for normal and adenoma  $\times 100$ , for CA and poorly differentiated  $\times 200$ . **(c)** Graph showing the intensity of HP1 $\alpha$  staining in PC ( $N=32$ ) compared with papillary carcinoma metastatic (PCM,  $N=3$ ) and FC ( $N=14$ ) versus follicular carcinoma metastatic (FCM,  $N=8$ ) from immunohistochemical staining of the human thyroid tumor TMA in **a**.

In general, ACIS brown staining intensity scores below 100 were equivalent to negative (0) staining by manual grading, 100–110 was equivalent to weak (1+) staining, 111–120 was equivalent to (2+) staining and  $>120$  was equivalent to (3+) strong nuclear reactivity.

The specificity of the antibodies that recognize HP1 $\beta$  and HP1 $\alpha$  was confirmed by immunoblot analysis using total protein extracted from three frozen advanced papillary carcinomas and a Hurthle cell variant, each showed a single band specific for the protein (Figure 2c). This analysis also confirmed the reduction of HP1 $\alpha$  and HP1 $\beta$  expression in

metastatic papillary carcinomas observed by immunohistochemistry.

### HP1 $\beta$ Expression is Altered in Thyroid Cells Overexpressing miR-205

Of the numerous miRNAs differentially upregulated in various histopathological types of thyroid tumors compared with normal tissue, miR-205 is predicted to target HP1 $\beta$  (TargetScanHuman, 2009).<sup>17,19</sup> We observed a strong negative correlation of miR-205 and HP1 $\beta$  expression (Pearson  $r = -0.52$ ) in previously published array data from

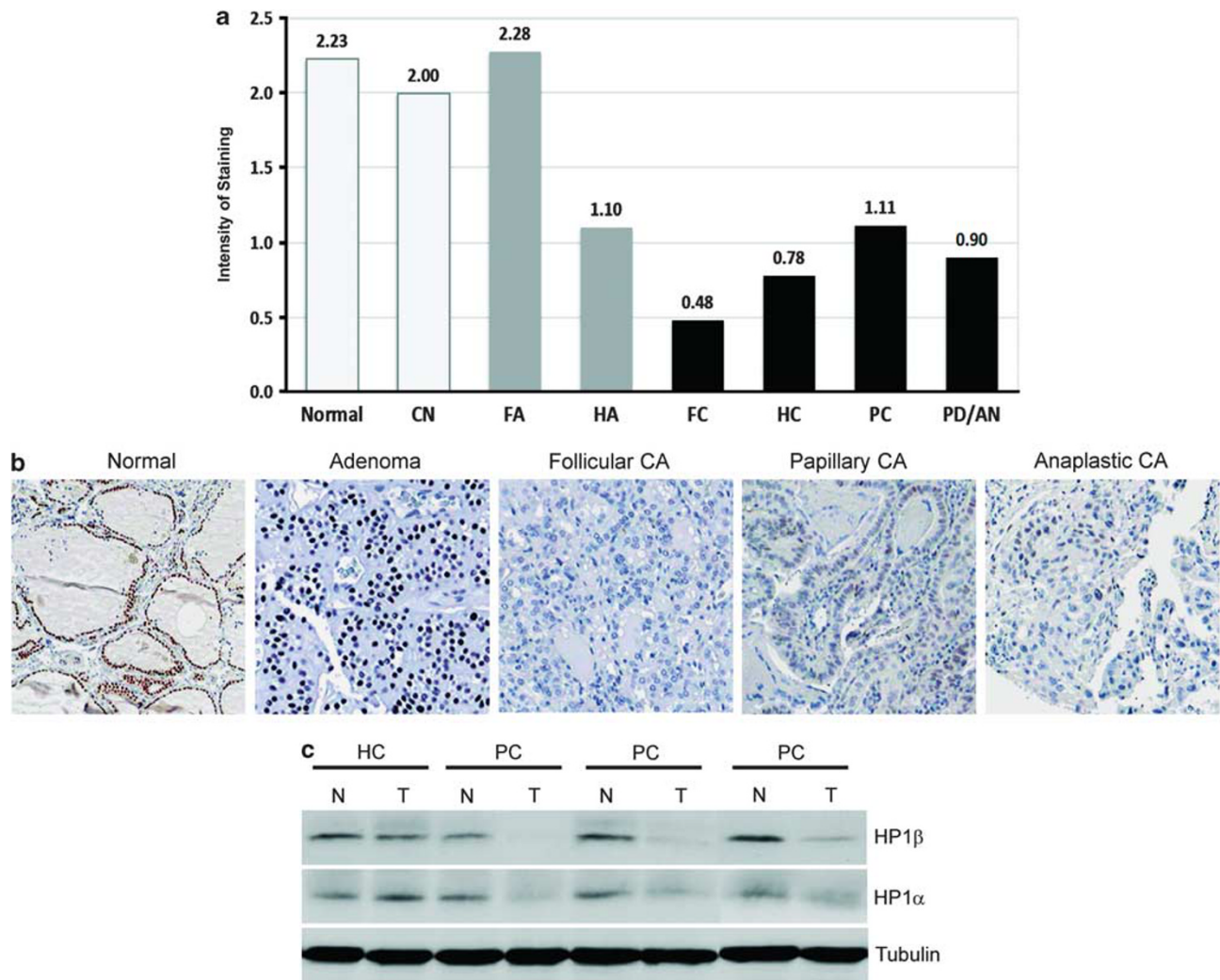


**Figure 2** Loss of HP1 $\beta$  expression occurs with increasing grade of thyroid tumor. (a) Graph showing the results from immunohistochemical staining of the 189 sample human thyroid tumor TMA for HP1 $\beta$ . The intensity of HP1 staining was graded as 0, 1+, 2+, and 3+. Colloid nodules (CN), follicular adenomas (FA), Hurthle cell adenomas (HA), follicular carcinomas (FC), Hurthle cell carcinomas (HC), papillary carcinomas (PC), poorly differentiated and anaplastic tumors (PD/AN), and normal adjacent thyroid tissue were stained. (b) Representative images from the immunohistochemical staining of the human thyroid tumor TMA are shown for HP1 $\beta$ . Haematoxylin counterstaining (blue) indicates nuclei, HP1 $\beta$ -positive nuclei (brown). CA, carcinoma. Original magnification  $\times 100$ . (c) Total protein isolated from three frozen advanced thyroid papillary carcinomas (PC) and a Hurthle cell carcinoma (HC) was analyzed by immunoblotting for expression of HP1 $\beta$  and HP1 $\alpha$  and  $\alpha$ -tubulin as a loading control. N, normal matched adjacent tissue, T, tumor tissue.

papillary carcinomas (Figure 3a).<sup>21</sup> These data show that miR-205 and HP1 $\beta$  were significantly up and down-regulated ( $P < 0.05$ ), respectively in these tumors. Not surprisingly though a negative correlation with HP1 $\beta$  expression was also observed for other upregulated miRNAs such as miR-10a (Pearson  $r = -0.73$ ) even though miR-10a is not predicted to target HP1 $\beta$ .<sup>19,22</sup> Therefore, to determine if increased expression of miR-205 can alter the level of endogenous HP1 $\beta$  protein, immortalized Nthy-ori 3-1 thyroid cells were transiently transfected with a selection of Pre-miR miRNA precursors that are processed by the cell into mature miRNAs. Cells overexpressing miR-205 showed reduced HP1 $\beta$  protein levels

compared with mock transfected cells and those transfected with a scrambled pre-miRNA precursor control (NC2) that does not have any predicted endogenous targets (Figure 3b). Overexpression of miR-200a, another miRNA predicted to target HP1 $\beta$  but with reduced complementarity to its seed region in the 3' UTR of HP1 $\beta$  compared with that of miR-205, only slightly reduced the level of endogenous HP1 $\beta$ . Both miR-10a and miR-223, not predicted to target HP1 $\beta$ , did not alter the level of endogenous HP1 $\beta$ . As a further control, none of the tested miRNAs were predicted to target HP1 $\alpha$  and, as shown in Figure 3b, they do not alter the level of endogenous HP1 $\alpha$  protein in these cells. Similar results were observed when these Pre-miR miRNAs were

**Table 1 Results of HP1 $\beta$  expression analysis by automated cell image analysis (ACIS)**

Histology	Group	No. of cases	HP1 $\beta$ %		HP1 $\beta$ intensity	
NT/CN	Normal	85	43.42	43.42	139.36	139.12
FA	Benign	18	63.39	51.18	129.72	120.21
HA		10	29.2		103.1	
FC	Malignant	22	13.62	24.48	79.5	98.62
HC		8	26.49		90	
PC		35	33.5		109	
PD/AC		11	17.94		113.3	
Total		189	$P < 0.001$		$P < 0.001$	

Abbreviations: CN, colloid nodule; FA, follicular adenoma; FC, follicular carcinoma, primary and metastatic; HA, Hurthle cell adenoma; HC, Hurthle cell carcinoma; PC, papillary carcinoma, primary and metastatic; PD/AC, poorly differentiated and anaplastic carcinoma; NT, normal thyroid tissue.

transiently transfected into HeLa cervical carcinoma cells (data not shown).

To determine if miR-205 post-transcriptionally regulates HP1 $\beta$  expression directly, we used a 3' UTR luciferase reporter assay. The 3' UTR region of the CBX1 (HP1 $\beta$ ) gene that is a predicted binding site for miR-205 was cloned into the 3' UTR of the pMIR-REPORT vector (Figure 4a). Nthy-ori 3-1 cells were co-transfected with this reporter vector (WT) or one where the putative HP1 $\beta$  3' UTR seed region has been altered to prevent binding of miR-205 (Mut), along with the pre-miRNA precursors. The transfection of pre-miRNA scrambled (NC2) and miR-10a precursors, which do not alter endogenous HP1 $\beta$  levels in Nthy-ori 3-1 cells (Figure 3b), demonstrated no difference in luciferase activity between the pMIR-REPORT-HP1 $\beta$  WT and Mut vectors (Figure 4b).

In the presence of miR-205, there was a 30% reduction ( $P < 0.05$ ) in luciferase activity in cells transfected with the pMIR-REPORT-HP1 $\beta$  vector containing the WT HP1 $\beta$  3' UTR region compared with the Mut sequence that prevents binding of miR-205 (Figure 4b). This suggests that the observed reduction in HP1 $\beta$  expression in thyroid tumors may in part be due to miR-205 downregulating HP1 $\beta$  post-transcriptionally by binding its 3' UTR.

## DISCUSSION

The altered expression of two HP1 isoforms during thyroid tumorigenesis is not surprising given thyroid cancers generally exhibit a loss of heterochromatin integrity at the microscopic level.<sup>1</sup> Thyroid carcinomas demonstrate a significant reduction in the level of HP1 $\beta$  compared with either normal tissue, proliferative colloid nodules, or benign follicular adenomas (Figure 2). The decrease in HP1 $\beta$

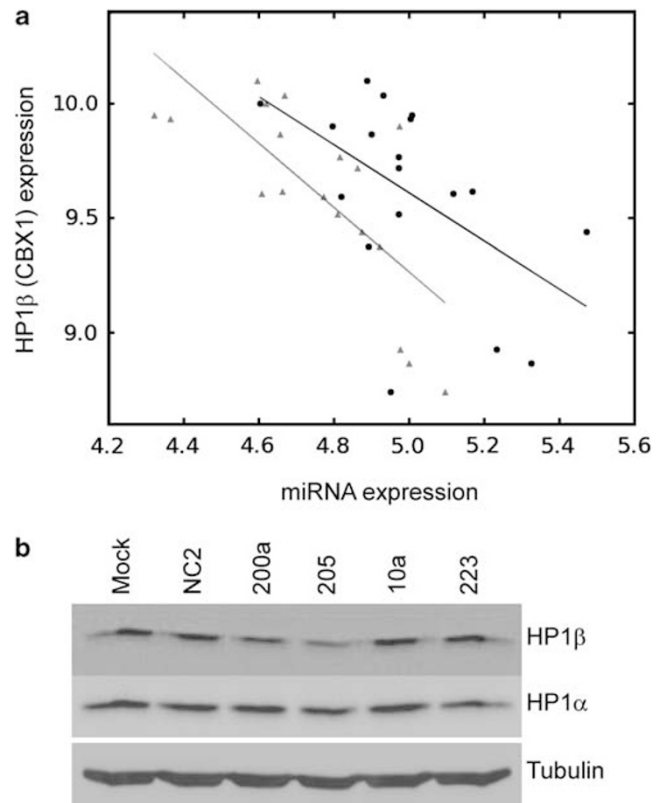


**Figure 3** Downregulation of endogenous HP1 $\beta$  expression by miR-205. (a) Expression values for miR-205 (closed circles) and miR-10a (gray triangles) are graphed against expression values for HP1 $\beta$  (CBX1 gene) of thyroid papillary carcinomas and normal tissue from published array data. (b) Nthy-ori 3-1 cells were transiently transfected with Pre-miR miRNA precursors for either a scrambled control miRNA (NC2), miR-200a, miR-205, miR-10a, miR-223 or without any Pre-miR miRNA precursor (Mock). Total protein was analyzed by immunoblot for expression of HP1 $\beta$ , HP1 $\alpha$  and  $\alpha$ -tubulin as a loading control.

expression between follicular adenoma and carcinoma groups was particularly dramatic (4.7-fold) and could have diagnostic implications. This downregulation of HP1 $\beta$  likely contributes to tumor progression, as knockdown of HP1 $\beta$  in cancer cell lines promotes chromatin disorganization, genomic instability and also increases their invasiveness.<sup>12,23</sup>

In contrast to the changes in HP1 $\beta$  expression, HP1 $\alpha$  levels in adenomas and non-metastatic carcinomas were comparable to or increased slightly from those in normal tissue (Figure 1). However, HP1 $\alpha$  expression was reduced in metastatic carcinomas from regional or distal sites. This corresponds with observations in breast tissue where non-invasive breast carcinomas were shown to have high levels of HP1 $\alpha$  protein,<sup>3</sup> whereas metastatic lesions from distant sites in the body had decreased levels of HP1 $\alpha$ .<sup>5</sup> This suggests that HP1 $\alpha$  has a role in suppressing metastasis and is supported by the overexpression of HP1 $\alpha$  decreasing the invasive potential of a breast cancer cell line.<sup>24</sup> Together these results show a differential loss of HP1 isoform expression

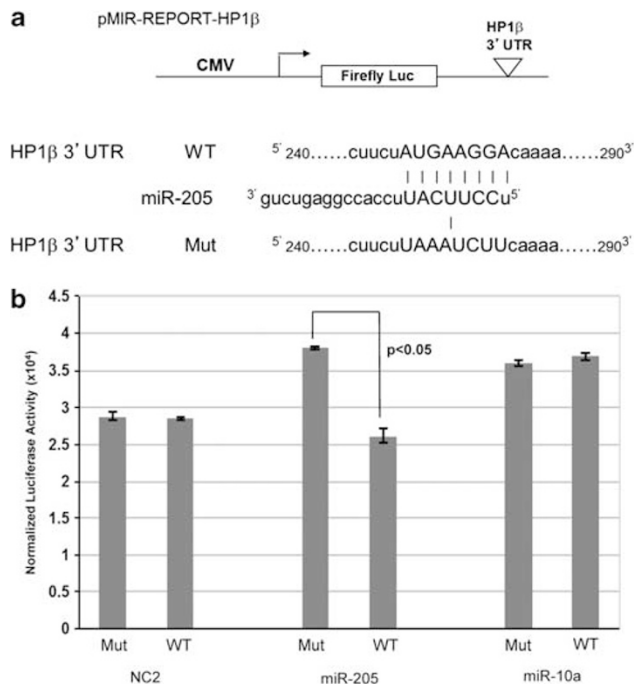


**Figure 4** Effects of miR-205 on a luciferase reporter gene bearing a 3' UTR segment of HP1 $\beta$ . **(a)** Schematic representation of the pMIR-REPORT-HP1 $\beta$  3' UTR vector. The CMV promoter drives the constitutive expression of firefly luciferase coding sequence with the region from 240 to 290 bp of the HP1 $\beta$  3' UTR sequence containing the predicted binding region of miR-205 cloned downstream of the luciferase gene. Shown below is the predicted seed match between miR-205 and the HP1 $\beta$  (CBX1) 3' UTR present in the pMIR-REPORT-HP1 $\beta$  WT vector and the mismatches present in pMIR-REPORT-HP1 $\beta$  Mut vector. **(b)** Nthy-ori 3-1 cells were co-transfected with either pMIR-REPORT-HP1 $\beta$  WT or Mut vectors, and the following Pre-miR miRNA Precursors: NC2, miR-205 or miR-10a, and the  $\beta$ -galactosidase control vector. Reporter activity was measured by luciferase assay and normalized to  $\beta$ -galactosidase.

during malignancy in thyroid tissue and preliminary immunohistochemical analyses suggests this pattern is common to other solid tumor types (data not shown).

How the expression of each HP1 isoform is downregulated is poorly understood. In thyroid tumors, reduced expression is unlikely to be due to a decrease in the copy number of HP1 $\beta$  CBX1) or HP1 $\alpha$  (CBX5) gene, as loss of 17q21.32 or 12q13.13, respectively, has not yet been observed.<sup>25–27</sup> MiR-205 has been shown to be significantly upregulated in papillary and anaplastic carcinomas compared with hyperplastic nodules and normal thyroid tissue.<sup>19</sup> As miR-205 can directly target the 3' UTR of HP1 $\beta$  (Figure 4b), loss of HP1 $\beta$  in these carcinomas could be due to miR-205 post-transcriptionally downregulating HP1 $\beta$  expression. This demonstrates that the expression of the HP1 isoforms could be regulated post-transcriptionally. Given that the reduction of HP1 $\beta$  is observed across a range of malignant thyroid lesions, it will be of interest to uncover other transcriptional and post-transcriptional regulators.

In summary, these results suggest that the differential expression of HP1 $\alpha$  and HP1 $\beta$  across benign and malignant tumors can be further explored as potential markers, when loss of HP1 $\beta$  and HP1 $\alpha$  can be interpreted in favor of malignancy or carcinoma with metastatic potential, respectively. It will be of interest to explore the contribution of the decreased expression of these HP1 isoforms to the pathogenesis and progression of thyroid carcinomas.

#### ACKNOWLEDGMENTS

This study was supported by grants from the Cancer Society of New Zealand and the Palmerston North Medical Research Foundation. We thank Bruce Lockett and Natisha Magan for critical reading of the manuscript.

#### DISCLOSURE/CONFLICT OF INTEREST

The authors declare no conflict of interest.

- Zink D, Fischer AH, Nickerson JA. Nuclear structure in cancer cells. *Nature Rev Cancer* 2004;4:677–687.
- Zeng W, Ball Jr AR, Yokomori K. HP1: heterochromatin binding proteins working the genome. *Epigenetics* 2010;5:287–292.
- De Koning L, Savignoni A, Boumendil C, *et al*. Heterochromatin protein 1alpha: a hallmark of cell proliferation relevant to clinical oncology. *EMBO Mol Med* 2009;1:178–191.
- Ritou E, Bai M, Georgatos SD. Variant-specific patterns and humoral regulation of HP1 proteins in human cells and tissues. *J Cell Sci* 2007;120(Pt 19):3425–3435.
- Kirschmann DA, Linger RA, Gardner LM, *et al*. Down-regulation of HP1Hsalpha expression is associated with the metastatic phenotype in breast cancer. *Cancer Res* 2000;60:3359–3363.
- Lieberthal JG, Kaminsky M, Parkhurst CN, *et al*. The role of YY1 in reduced HP1alpha gene expression in invasive human breast cancer cells. *Breast Cancer Res* 2009;11:R42.
- Pomeroy SL, Tamayo P, Gaasenbeek M, *et al*. Prediction of central nervous system embryonal tumour outcome based on gene expression. *Nature* 2002;415:436–442.
- Thomsen R, Christensen DB, Rosborg S, *et al*. Analysis of HP1alpha regulation in human breast cancer cells. *Mol Carcinog* 2011;50: 601–613.
- Wasenius VM, Hemmer S, Kettunen E, *et al*. Hepatocyte growth factor receptor, matrix metalloproteinase-11, tissue inhibitor of metalloproteinase-1, and fibronectin are up-regulated in papillary thyroid carcinoma: a cDNA and tissue microarray study. *Clin Cancer Res* 2003;9:68–75.
- Takanashi M, Oikawa K, Fujita K, *et al*. Heterochromatin protein 1gamma epigenetically regulates cell differentiation and exhibits potential as a therapeutic target for various types of cancers. *Am J Pathol* 2009;174:309–316.
- Shapiro E, Huang H, Ruoff R, *et al*. The heterochromatin protein 1 family is regulated in prostate development and cancer. *J Urol* 2008;179:2435–2439.
- Tell R, Rivera CA, Eskra J, *et al*. Gastrin-releasing peptide signaling alters colon cancer invasiveness via heterochromatin protein 1Hsbeta. *Am J Pathol* 2011;178:672–678.
- Nishimura K, Hirokawa YS, Mizutani H, *et al*. Reduced heterochromatin protein 1-beta (HP1beta) expression is correlated with increased invasive activity in human melanoma cells. *Anticancer Res* 2006;26: 4349–4356.
- Wynford-Thomas D. Origin and progression of thyroid epithelial tumours: cellular and molecular mechanisms. *Horm Res* 1997;47: 145–157.
- Hedinger C, Williams ED, Sobin LH. The WHO histological classification of thyroid tumors: a commentary on the second edition. *Cancer* 1989;63:908–911.
- Nikiforova MN, Nikiforov YE. Molecular diagnostics and predictors in thyroid cancer. *Thyroid* 2009;19:1351–1361.
- Marini F, Luzi E, Brandi ML. MicroRNA role in thyroid cancer development. *J Thyroid Res* 2011;2011:407123.

18. Nikiforova MN, Chiosea SI, Nikiforov YE. MicroRNA expression profiles in thyroid tumors. *Endocr Pathol* 2009;20:85–91.
19. Nikiforova MN, Tseng GC, Steward D, *et al*. MicroRNA expression profiling of thyroid tumors: biological significance and diagnostic utility. *J Clin Endocrinol Metab* 2008;93:1600–1608.
20. Tretiakova M, Turkyilmaz M, Grushko T, *et al*. Topoisomerase IIalpha in Wilms' tumour: gene alterations and immunoexpression. *J Clin Pathol* 2006;59:1272–1277.
21. He H, Jazdzewski K, Li W, *et al*. The role of microRNA genes in papillary thyroid carcinoma. *Proc Natl Acad Sci USA* 2005;102:19075–19080.
22. Tetzlaff MT, Liu A, Xu X, *et al*. Differential expression of miRNAs in papillary thyroid carcinoma compared to multinodular goiter using formalin fixed paraffin embedded tissues. *Endocr Pathol* 2007; 18:163–173.
23. Aucott R, Bullwinkel J, Yu Y, *et al*. HP1-beta is required for development of the cerebral neocortex and neuromuscular junctions. *J Cell Biol* 2008;183:597–606.
24. Norwood LE, Moss TJ, Margaryan NV, *et al*. A requirement for dimerization of HP1Hsalpha in suppression of breast cancer invasion. *J Biol Chem* 2006;281:18668–18676.
25. Wreesmann VB, Ghossein RA, Hezel M, *et al*. Follicular variant of papillary thyroid carcinoma: genome-wide appraisal of a controversial entity. *Genes Chromosomes Cancer* 2004;40:355–364.
26. Wreesmann VB, Ghossein RA, Patel SG, *et al*. Genome-wide appraisal of thyroid cancer progression. *Am J Pathol* 2002;161: 1549–1556.
27. Hemmer S, Wasenius VM, Knuutila S, *et al*. DNA copy number changes in thyroid carcinoma. *Am J Pathol* 1999;154:1539–1547.